

STATISTICS OF MULTIPLE EXTRANEIOUS SIGNALS ON A COMPACT RANGE

John R. Jones and Esko A. Jaska

Microwave and Antenna Technology Development Laboratory
Georgia Tech Research Institute
Georgia Institute of Technology
Atlanta, GA 30332

*Sponsored by US Army EC
Fort Huachuca, AZ*

Abstract

Multiple mechanisms for the generation of extraneous signals exist in a compact range. These include edge diffraction, scattering from surface imperfections, direct feed radiation, and scattering from absorber or other objects in the range. The field quality in the quiet zone is the resultant of the direct signal and these multiple scattering mechanisms.

Since the scattering mechanisms are independent, their effects are often modeled independently and statistically combined to yield an estimate of quiet zone field quality. This paper examines the statistics of multiple independent extraneous signals in a compact range. It is shown that the amplitude ripple produced by an extraneous signal computed as the root sum of the squares (RSS) of the individual extraneous signals does not correctly predict the final quiet zone amplitude ripple.

Theoretical results for scattering from multiple thin gaps in the surface of a compact range are presented and statistical computer models are used to demonstrate the computation of the resultant compact range quiet zone.

Keywords: compact range, gap scattering,
statistical modeling

I. INTRODUCTION

The field in the quiet zone of a compact range is the superposition of the geometrical optics field from the reflector (the desired collimated field) and the scattered or extraneous fields from imperfections in the range. These imperfections include the edges of the reflector, which are often modified to reduce diffraction into the quiet zone; surface errors in the reflector; gaps between the panels of a panelized reflector; direct feed radiation into the quiet zone; scattering from objects in the range; and other mechanisms. It is necessary in the design of a compact range to estimate the effects of extraneous fields on the quiet zone field quantity. This entails modeling the effects of imperfections in the range.

Many of these effects are most usefully modeled statistically. That is to say, the effects of a single isolated extraneous signal source on the quiet zone field are computed by electromagnetic scattering analysis methods (Maxwell's equations, method of moments, GTD, etc.). The number and magnitudes of the extraneous signal

sources are estimated by examination of the manufacturing processes and tolerances. A statistical estimate of the extraneous signal magnitude associated with all instances of each mechanism is computed and the resulting estimates for all extraneous signal generating mechanisms are statistically combined to produce a statistical description of the expected field quality for the range.

It is the statistics of combining extraneous signals arising from various mechanisms which is the subject of this paper. We will show that an approximate Rayleigh distribution closely models the resultant amplitude of even a modest number of extraneous signals resulting from panel gap scattering. Also, we compute the difference between this estimate and the usual RSS estimate for an example of compact range panel gap scattering.

II. THEORETICAL DEVELOPMENT

We will use as our example case prediction of the compact range quiet zone ripple caused by the gaps between the panels of a panelized reflector. Joy and Black [1] have analyzed this case in some detail. Using a method due to Butler [2], they compute the scattering from a single gap in an infinite parabolic cylinder relative to the incident illumination amplitude. This is analogous to the situation of a compact range with long gaps.

Given the constraints on the construction of the reflector we want to design, we can approximate the number of gaps that will be present in the reflector when it is constructed, and obtain an upper bound for their widths. We assume that our reflector has N gaps and that we know the widths and center coordinates of each one. The reflector and the gaps are infinitely long in the y -direction. This cylindrical geometry is shown in Figure 1.

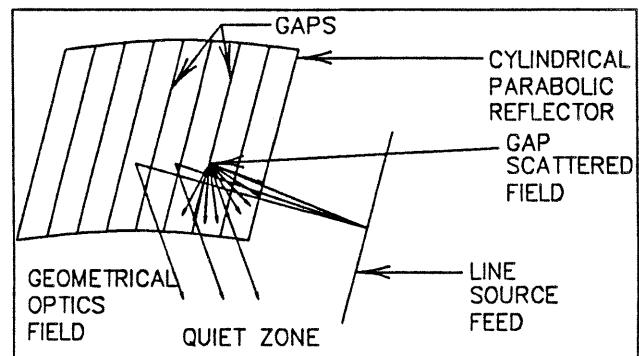


Figure 1. Cylindrical Reflector Geometry Analyzed by Joy and Black [1]

If we know the widths and locations of all the gaps, we can in principle compute the illumination on each gap, the scattering from each gap, and the resultant scattered field at the field point for each gap. By computing the field at each point in the quiet zone, we can precisely characterize the extraneous signal magnitude in the quiet zone by superposition.

This is usually not done because it is too computationally intensive and because the locations and widths of the panel gaps are not precisely known. What is usually done is to take the root-sum-of-the-squares (RSS) for the magnitude of the scattered field from the observed number of panel gaps to derive an expected extraneous signal magnitude in the quiet zone. It is then assumed that somewhere in the quiet zone the extraneous signal will reinforce the geometrical optics (GO) field, and somewhere the two fields will tend to cancel as shown in Figure 2. Our method of analysis departs from this in that we use a more accurate method of statistically combining the scattered fields to predict the expected extraneous signal magnitude.

To obtain a worst case estimate, we let all the gaps have the same width W_{\max} . Then the gap scattered fields will all have the same amplitude in the quiet zone

$E_{s_{\max}} \cong E_s$. Now we let the phases of the gap scattered

fields, φ_{sn} , be described by a uniform distribution from $-\pi$ to π . The probability density function for the phase of each gap scattered field is given by

$$p_{\varphi_m}(\varphi) = \begin{cases} \frac{1}{2\pi} & -\pi < \varphi < \pi \\ 0 & \text{otherwise} \end{cases} \quad (1)$$

Note that for a given compact range the phases of the gap scattered fields are not random at all, but (in principle) deterministic. Taken over the ensemble of "possible" compact ranges however, equation (1) is a valid description. This ensemble of "possible" compact ranges is the sample space of which any constructed compact range is a member. Therefore, in designing a compact range, it is the statistics of this ensemble which must be considered.

For each gap, we write the gap scattered field as

$$\hat{E}_{sn} = E_s e^{j\varphi_{sn}} = E_s (\cos\varphi_{sn} + j\sin\varphi_{sn}) \quad (2)$$

The caret (^) denotes a phasor quantity and we consider only one polarization component of the field without loss of generality. The magnitude of the gap scattered field is written as $|\hat{E}_{sn}| = E_s$. Now the total scattered field at a point is just the superposition of all the scattered fields.

$$\hat{E}_T = \sum_{n=1}^N (E_s \cos\varphi_{sn} + jE_s \sin\varphi_{sn}) \quad (3)$$

or

$$\hat{E}_T = E_s \left[\sum_{n=1}^N (\cos\varphi_{sn} + j\sin\varphi_{sn}) \right] \quad (4)$$

$$= E_s \left[\sum_{n=1}^N \cos\varphi_{sn} + j \sum_{n=1}^N \sin\varphi_{sn} \right] \quad (5)$$

The magnitude of the total field is given by

$$|\hat{E}_T| = E_s \sqrt{\left(\sum_{n=1}^N \cos\varphi_{sn} \right)^2 + \left(\sum_{n=1}^N \sin\varphi_{sn} \right)^2} \quad (6)$$

The quantities $\sum_{n=1}^N \cos\varphi_{sn}$ and $\sum_{n=1}^N \sin\varphi_{sn}$

are not really independent random variables, but if N is large enough they are distributed approximately as if they were independent Gaussian random variables.

It is well known that if x and y are independent Gaussian random variables with $\bar{x}=0$ and $\bar{y}=0$ and equal variances σ^2 , then for a random variable R defined as

$$R = \sqrt{x^2 + y^2} \quad (7)$$

the probability density function is [3]

$$p_R(r) = \begin{cases} \frac{r}{\sigma^2} \exp\left[-\frac{r^2}{2\sigma^2}\right] & r \geq 0 \\ 0 & r < 0 \end{cases} \quad (8)$$

This is the Rayleigh probability density function. It is shown in Figure 3 for two values of σ^2 . This is the case we have (approximately) for compact range gap scattering.

We will set aside for the moment questions on the validity of the assumption that the random

variables $\sum_{n=1}^N \cos\varphi_{sn}$ and $\sum_{n=1}^N \sin\varphi_{sn}$ behave as if they

were independent. The simulations shown later indicate that for N sufficiently large, they do behave this way. We now focus on the distributions of these two random variables.

First we need the distributions of $\cos\varphi_{sn}$ and $\sin\varphi_{sn}$. The developments are identical. Consider the random variable

$$y = \cos\varphi_{sn} \quad (9)$$

We know the density function $p_{\varphi_{sn}}$ for φ_{sn} . To get the density function $p_{\cos\varphi_{sn}}$ for $\cos\varphi_{sn}$, we solve equation (9) for φ_{sn} at each value of y . The solutions are

$$\varphi_{sn} = \left. \begin{array}{l} \cos^{-1}(y) + 2n\pi \\ -\cos^{-1}(y) - 2n\pi \end{array} \right\} \quad n \text{ an integer} \quad (10)$$

Since $p_{\varphi_{sn}} = 0$ for $|\varphi| > \pi$, however, only the solutions with $n=0$ are important. There are therefore two solutions for φ_{sn} for each y ,

$$\begin{aligned} \varphi_{sn}^1 &= \cos^{-1}(y) \\ \varphi_{sn}^{-1} &= -\cos^{-1}(y) \end{aligned} \quad (11)$$

Since φ_{sn} is real, y assumes values only between -1 and 1. We can now write [4]

$$p_y(y) = \frac{p_{\varphi_{sn}}(\varphi_{sn}^1)}{|\cos'(\varphi_{sn}^1)|} + \frac{p_{\varphi_{sn}}(\varphi_{sn}^{-1})}{|\cos'(\varphi_{sn}^{-1})|} \quad (12)$$

For all φ from $-\pi$ to π , $p_{\varphi_{sn}}(\varphi) = \frac{1}{2\pi}$. The denominator is given by

$$\begin{aligned} \cos'(\pm\cos^{-1}(y)) &= -\sin(\pm\cos^{-1}(y)) \\ &= -\sqrt{1-y^2} \end{aligned} \quad (13)$$

So

$$\begin{aligned} p_y(y) &= \frac{1}{2\pi} \frac{1}{\sqrt{1-y^2}} + \frac{1}{2\pi} \frac{1}{\sqrt{1-y^2}} \\ &= \frac{1}{\pi\sqrt{1-y^2}} \end{aligned} \quad (14)$$

Now we can compute the mean and standard deviation of $y = \cos\varphi_{sn}$.

$$\begin{aligned} \bar{y} &= \int_{-1}^{+1} y p_y(y) dy = \int_{-1}^{+1} \frac{y}{\pi\sqrt{1-y^2}} dy \\ &= \frac{1}{\pi} \left(-\sqrt{1-y^2} \right) \Big|_{-1}^{+1} = 0 \end{aligned} \quad (15)$$

So $y = \cos\varphi_{sn}$ has zero mean. Also,

$$\begin{aligned} \sigma_y^2 &= \int_{-1}^{+1} (y-\bar{y})^2 p_y(y) dy \\ &= \int_{-1}^{+1} y^2 \cdot \frac{1}{\pi\sqrt{1-y^2}} dy \\ &= \frac{1}{\pi} \left[\frac{-y}{2} \sqrt{1-y^2} + \frac{1}{2} \sin^{-1}(y) \right]_{-1}^{+1} \\ &= \frac{1}{2} \end{aligned} \quad (16)$$

So we now have the mean and standard deviation for $y = \cos\varphi_{sn}$. By an identical derivation we get identical results for $z = \sin\varphi_{sn}$.

By the Central Limit Theorem, for N sufficiently large,

a random variable $W = \sum_{n=1}^N x_n$ approaches Gaussian if the distributions of the random variables x_n satisfy certain broad conditions [4]. The random variables y and z defined above satisfy these conditions and so the random variables $\sum_{n=1}^N \cos\varphi_{sn}$ and $\sum_{n=1}^N \sin\varphi_{sn}$ tend to Gaussian distributions. Then, if they are independent (or if they behave as if they are), $|\hat{E}_T|$ tends to a Rayleigh distribution.

The distribution of the magnitude of \hat{E}_T , the total scattered field, will peak at $E_s \sqrt{\frac{N}{2}}$. The mean of $|\hat{E}_T|$

is given by $|\hat{E}_T| = E_s \frac{\sqrt{N\pi}}{2}$ and the variance by

$\sigma_{|\hat{E}_T|}^2 = 0.429 E_s^2 \frac{N}{2}$. For a Rayleigh distribution, 99.7% of the points will lie less than about 5.18 standard deviations from the origin.

III. NUMERICAL EXAMPLE

For our numerical example, we choose a range design with 20 long gaps with a maximum width of 0.06". This case was analyzed at 6 GHz by Black and Joy. They compute the maximum scattered field for a single gap as -46.6 dB relative to the incident field at 6 GHz. Thus, for a single gap,

$$|\hat{E}_s| = 4.67 \times 10^{-3}. \quad (17)$$

If there are 20 gaps, taking the RSS of the magnitudes yields

$$|\hat{E}_T| = \sqrt{20}|\hat{E}_s| = 20.92 \times 10^{-3} \quad (18)$$

$$|\hat{E}_T|_{dB} = -33.6 \text{ dB}$$

relative to the incident illumination. Assuming that this reinforces the GO field somewhere and cancels it somewhere else in the quiet zone, this would lead to a predicted quiet zone ripple of 0.36 dB (± 0.18 dB).

The Rayleigh model for combining the fields predicts the field intensities and dB ripple shown in Table I. These results are for the same -46.6 dB maximum scattered amplitude with 20 gaps as that computed above.

TABLE I

RESULTS OF MULTIPLE GAP SCATTERING ANALYSIS		
	Field Intensity	dB Ripple
Most Likely	14.79×10^{-3}	0.257 dB ($\pm .123$ dB)
Mean	18.54×10^{-3}	0.322 dB ($\pm .161$ dB)
99.7% Confidence Level	50.5×10^{-3}	0.878 dB ($\pm .439$ dB)

The table shows that the mean and the most likely (highest probability) values for the scattering from 20 gaps are actually somewhat smaller than the ripple computed from the RSS gap scattered field. There is a long "tail" on the distribution which indicates the possibility of higher values of total scattered field.

IV. Simulation of the Distribution

Because the random variables describing the gap scattered fields are not all independent, the above analysis is not rigorously correct. Even so, simulations of the field intensity for multiple gaps indicate that it is a useful approximation.

Figure 4 shows a graph of the frequency of $|\hat{E}_{sT}|$ for 1,000,000 random draws. The resemblance of the relative frequency curve to the Rayleigh probability density is unmistakable. Figure 5 shows a comparison of the computed Rayleigh probability density (theory) and the simulated data. As the figure shows, the curve shapes are very similar. Finally, Figure 6 shows the actual resultant complex field amplitudes for the simulation. As the figure indicates, the distribution is concentrated in an annulus about the origin. The distribution of Figures 4 and 5 yields the distribution of Figure 6 when the "uniform" ϕ -distribution is integrated out.

V. SUMMARY AND CONCLUSIONS

The scattering from multiple gaps in a compact range has been shown to correspond closely to a Rayleigh distribution. This indicates that it is possible for the total scattered field from multiple gaps to be higher than the RSS of the individual scattered fields. This same analysis should apply to other multiple scattering mechanisms as well.

VI. REFERENCES

1. D. N. Black and E. B. Joy, "A Model for the quiet zone effect of gaps in compact range reflectors" in Proceedings of the 10th Annual Meeting of the Antenna Measurement Techniques Association, Atlanta, Georgia: Antenna Measurement Techniques Association, 1988, pp. 9-15 - 9-20.
2. C. M. Butler, "General solutions of the narrow strip (and slot) integral equations," IEEE Trans. Antennas Propagat., vol. AP-32, no. 12, pp. 1327-1335, Dec. 1984.
3. G. R. Cooper and C. D. McGillem, Probabilistic Methods of Signal and System Analysis. New York: Holt, Rinehart and Winston, Inc., 1971.
4. A. Papoulis, Probability, Random Variables and Stochastic Processes. New York: McGraw-Hill, 1965.

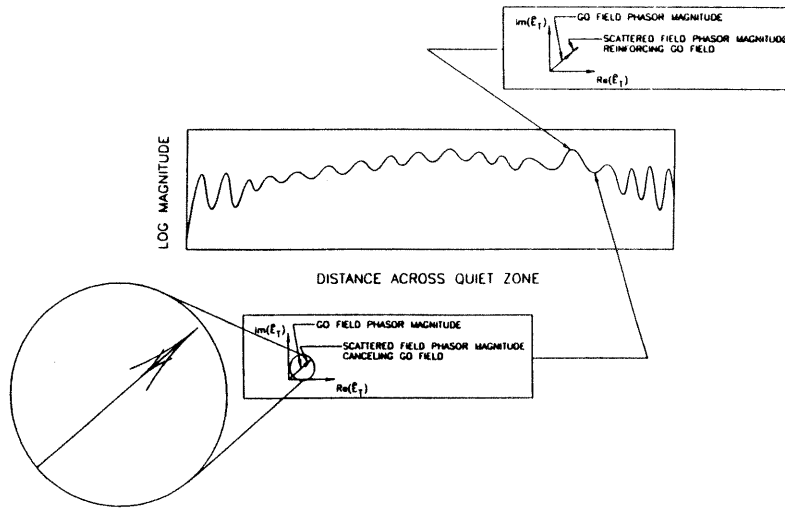


Figure 2. Phasor Summation of the Geometrical Optics (GO) Field and Gap Scattered Field

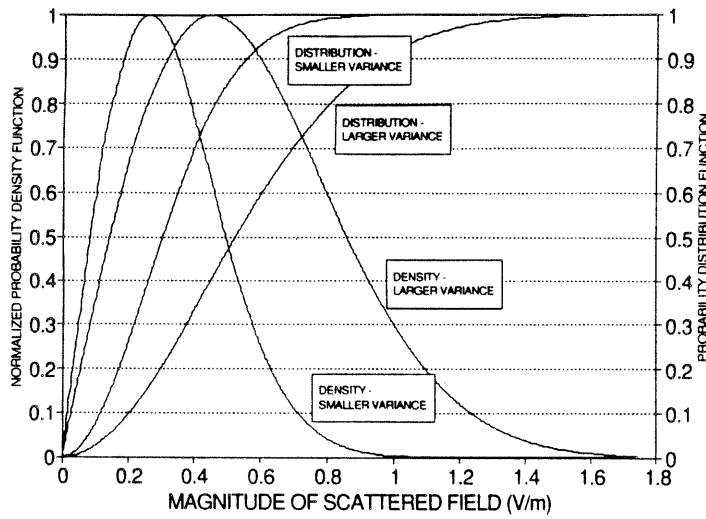


Figure 3. Sample Rayleigh Probability Density and Distribution Functions

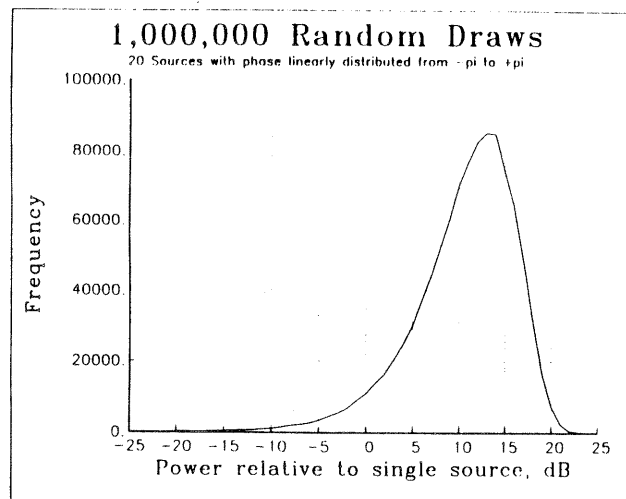


Figure 4. Simulation of Compact Range Gap Scattering

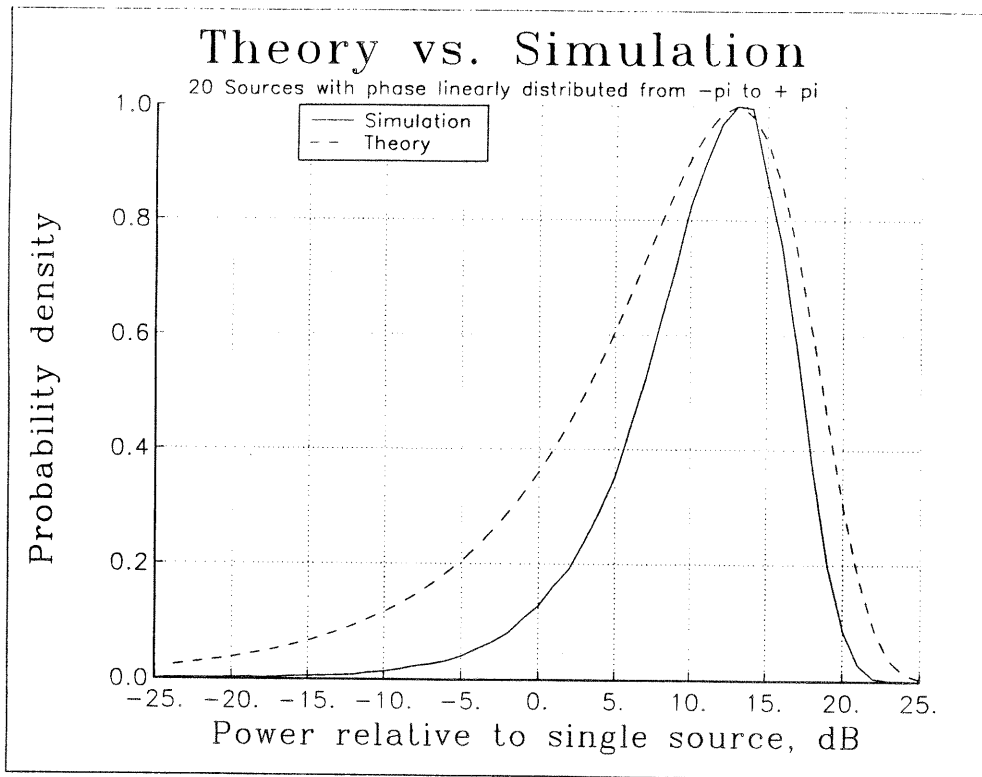


Figure 5. Simulation of Compact Range Gap Scattering (Simulation) vs. Normalized Rayleigh Probability Density (Theory)

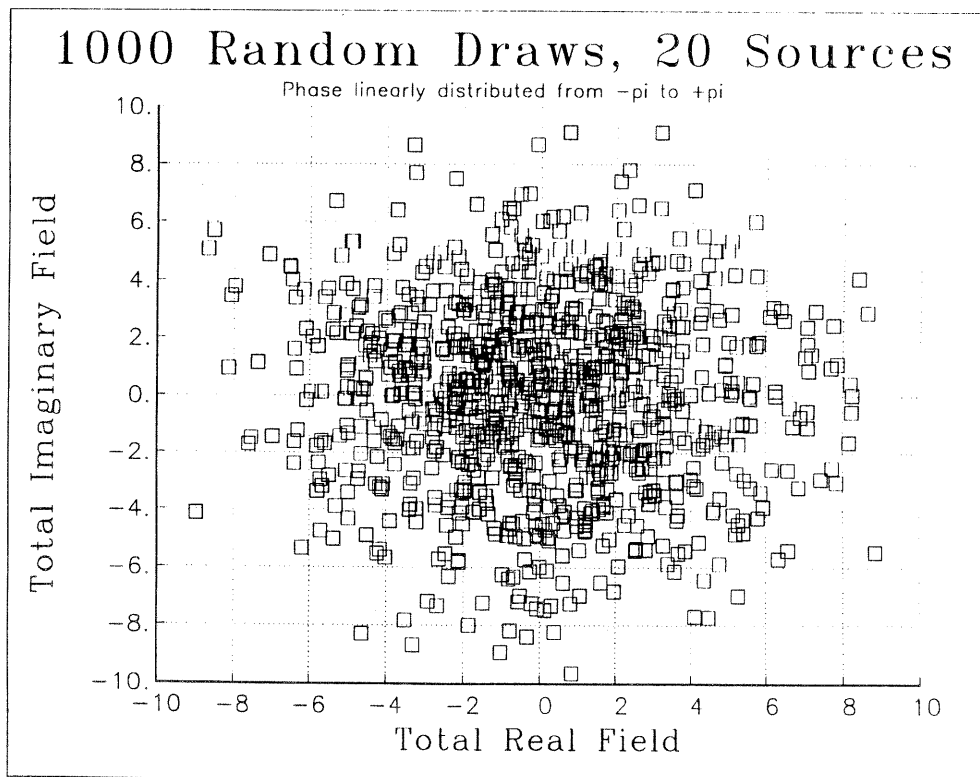


Figure 6. Total Scattered Field Scatter Diagram